HHS Public Access

Author manuscript

Neuron. Author manuscript; available in PMC 2017 May 04.

Published in final edited form as:

Neuron. 2016 May 4; 90(3): 581–595. doi:10.1016/j.neuron.2016.03.017.

Drosophila SLC22A transporter is a memory suppressor gene that influences cholinergic neurotransmission to the mushroom bodies

Yunchao Gai[*], **Ze Liu**[*], **Isaac Cervantes-Sandoval**, and **Ronald L. Davis**

Department of Neuroscience, The Scripps Research Institute Florida, Jupiter, Florida 33458, USA

SUMMARY

The mechanisms that constrain memory formation are of special interest because they provide insights into the brain's memory management systems and potential avenues for correcting cognitive disorders. RNAi knockdown in the *Drosophila* mushroom body neurons (MBn) of a newly discovered memory suppressor gene, Solute Carrier DmSLC22A, a member of the organic cation transporter family, enhances olfactory memory expression, while overexpression inhibits it. The protein localizes to the dendrites of the MBn, surrounding the presynaptic terminals of cholinergic afferent fibers from projection neurons (Pn). Cell-based expression assays show that this plasma membrane protein transports cholinergic compounds with the highest affinity among several *in vitro* substrates. Feeding flies choline or inhibiting acetylcholinesterase in Pn enhances memory; an effect blocked by overexpression of the transporter in the MBn. The data argue that DmSLC22A is a memory suppressor protein that limits memory formation by helping to terminate cholinergic neurotransmission at the Pn:MBn synapse.

INTRODUCTION

Genetic studies have now identified hundreds of genes required for normal memory formation. Some of these genes regulate the development of the cells and circuits required for learning; some mediate the physiological changes that occur with acquisition and storage (Murakami, 2007; Havekes and Abel, 2009; Ardiel and Rankin, 2010; Tomchik and Davis, 2013; Walkinshaw et al., 2015). Of particular interest are gene functions that suppress

Corresponding author: Ronald L. Davis, Department of Neuroscience, The Scripps Research Institute Florida, Jupiter, Florida 33458, USA, 561-228-3463, ; Email: rdavis@scripps.edu

*These authors made equal contributions

SUPPLEMENTAL INFORMATION

Supplemental Information includes Supplemental Experimental Procedures, eight figures, two tables, and one movie and can be found with this article online at http://xxxxxxxxxxx.

AUTHOR CONTRIBUTIONS

Y.G., Z.L, I.C-S. and R.L.D. together conceptualized and designed all experiments. Y.G. performed all of the behavioral and Western blotting experiments. Y.G. and Z.L. performed the transport assays. Z.L. performed the immunohistochemistry experiments. I.C-S. performed the functional imaging. Y.G., Z.L. and I.C.-S. analyzed the data from their corresponding experiments. All authors discussed the data included in the manuscript.

normal memory formation and by analogy with tumor suppressor genes, are referred to as memory suppressor genes (Abel et al., 1998). These genes and their products can, in principle, suppress memory formation by antagonizing the process of acquisition, limiting memory consolidation, promoting active forgetting, or inhibiting retrieval. Recently, we completed a large RNAi screen of ~3500 *Drosophila* genes and identified several dozen new memory suppressor genes (Walkinshaw et al., 2015), identified as such, because RNAi knockdown produces an enhancement in memory performance after olfactory conditioning.

Aversive olfactory classical conditioning is a well-studied type of learning in *Drosophila* and consists of learning a contingency between an odor conditioned stimulus (CS) and most often an unconditioned stimulus (US) of electric shock. Many cell types in the olfactory nervous system are engaged in this type of learning (Tomchik and Davis, 2013; Guven-Ozkan and Davis, 2014), including antennal lobe projection neurons (Pn), several different types of mushroom body neurons (MBn), dopamine neurons (DAn) and others, but a focused model of olfactory memory formation holds that MBn are integrators of CS and US information with the CS being conveyed to the MBn dendrites by the axons of cholinergic, excitatory Pn of the antennal lobe, and the US conveyed to the MBn by DAn (Davis, 1993; Tomchik and Davis, 2013; Guven-Ozkan and Davis, 2014).

A memory suppressor gene that we identified and describe in this report encodes a member of the SLC22A transporter family. The Solute Carrier (SLC) family of transporters in humans consists of 395 different, membrane-spanning transporters that have been organized into 52 different families (Lin et al., 2015). Some of these are localized pre-synaptically and involved in neurotransmitter recycling, others localize to glia for clearance of neurotransmitter from the synapse. In addition, glutamate transporters can be localized post-synaptically to regulate neurotransmission strength via clearance mechanisms (Vandenberg and Ryan, 2013). Some of these SLC transporters have prominent roles in neurological and psychiatric disorders and in drug design, including SLC1A family members that are responsible for glutamate uptake and clearance of this neurotransmitter from the synaptic cleft and SLC6A2-4 proteins that transport monoamines into cells (Blakely and Edwards, 2012). Inhibitors of these proteins, which include the serotonin specific reuptake inhibitors (SSRIs) and serotonin-noradrenaline reuptake inhibitors (SNRIs) increase monoamine dwell time at the synapse and are used to treat depression and several other neuropsychiatric disorders (Lin et al., 2015).

The SLC22A family of transporters is distinguished into two major classes that carry either organic cations (SLC22A1-5, 15, 16 and 21) or anions (SLC22A6-13 and 20) across the plasma membrane, with generally low substrate binding affinity and high capacity (Sturm et al., 2007; Koepsell, 2013b). They transport numerous molecules with diverse structures (Koepsell and Endou, 2004; Koepsell, 2013a), including drugs, acetylcholine, dopamine, histamine, serotonin, and glycine among others (Koepsell, 2013b). Ergothioneine has been identified as a high affinity substrate for SLC22A4 and spermidine for SLC22A16 (Nakamura et al., 2007; Aouida et al., 2010). Mice mutant in the two organic cation transporters, SLC22A2 and SLC22A3, exhibit behavioral phenotypes suggestive of functions in anxiety, stress and depression (Courousse and Gautron, 2015). These observations point the importance of the SLC22A family for brain function and cognition.

Recently, a *Drosophila* SLC22A family member, *CarT* (CG9317) was identified and found to transport carcinine into photoreceptor neurons for the recovery of essential visual neurotransmitter histamine (Stenesen et al., 2015).

Here we show that the *Drosophila* gene, CG7442, functions as a memory suppressor gene and is a member of the SLC22A family. This transporter is expressed most abundantly in the dendrites of the MBn, at the synapses with the cholinergic antennal lobe Pn. Cell-based expression assays show that *Drosophila* SLC22A transports choline and acetylcholine with the highest affinity among several substrates. Pharmacological and genetic data support the model that *Drosophila* SLC22A functions at the Pn:MBn synapse to terminate cholinergic neurotransmission, differing from well-characterized presynaptic choline transporters for neurotransmitter recycling, and mechanistically explaining its role in behavioral memory suppression.

RESULTS

Drosophila CG7442 is a memory suppressor gene functioning in MBn and DAn

One of the memory suppressor genes identified in the aforementioned RNAi screen is *Drosophila* CG7442 (Walkinshaw et al., 2015). Flies expressing CG7442 RNAi-1 (RNAi-1 = line 106555) throughout the nervous system using the pan-neuronal driver *Nsyb-gal4* displayed significant memory enhancement compared to control genotypes (Figure 1A). We found that strong and broad knockdown of CG7442 using *tubulin-gal4* was lethal, and therefore focused on tissue-specific, RNAi knockdown approaches to provide the desired loss of function condition.

We employed a panel of *gal4* lines with cell type- or region-specific expression in the brain to map the memory suppressor function of CG7442. Bigenic progeny, each group containing a *gal4* driver along with CG7442 RNAi-1, were trained with odor paired with electric shock and tested for memory at 3h after conditioning. Each bigenic group was compared to its *gal4* control made heterozygous with the RNAi-1 parental line (60100). The 60100 line used for docking RNAi-based transgenes contains a P{attP,y^+,$w^{3'}$}VIE-260B insertion at a site selected based on its low level of basal expression and consistent high level of *gal4*-dependent expression across a range of tissues (http://flybase.org/reports/FBrf0208510.html). Thus, the 60100 genotype mated with the relevant *gal4* line offers an excellent control for pairwise comparison with flies expressing RNAi's from the docking site.

Memory of the conditioned aversive event was enhanced with CG7442 knockdown using multiple drivers that specifically express in the MBn or in DAn (Figure 1A). Memory remained unaltered relative to the control when the RNAi was expressed in DPMn, antennal lobe Pn, neurons of the central complex (CCn), MB-V2 neurons (MB-V2n), or glial cells (Figure 1A). We reproduced the memory enhancement with MBn knockdown in multiple independent experiments, and confirmed that memory enhancement required both *gal4* and *RNAi* transgenes (Figure 1B). We also employed other RNAi transgenes (RNAi-2 and RNAi-3) targeting different sequences of the CG7442 mRNA to ensure that the effects of RNAi-1 were specific to the CG7442 gene product. These two additional RNAi's produced

memory enhancement when driven with MBn or DAn *gal4* drivers (Figure 1C). Moreover, we expressed CG7442 RNAi-1 in three major types of MBn, α/β, α′/β′ and γ, which revealed that the memory suppressor function maps to both α/β and α′/β′ MBn (Figure 1D). Tests for sensory perception of odors and shock failed to show any significant difference between the control and experimental genotypes (Table S1). We conclude from these experiments that knockdown of CG7442 specifically in the α/β and α′/β′ MBn, or DAn, enhances olfactory memory expression when tested 3h after conditioning.

We verified the effect of RNAi-induced knock down of expression by both quantitative RT-PCR (qRT-PCR) and Western blotting using a polyclonal antibody raised in guinea pigs against the CG7442 protein product. Our qRT-PCR experiments showed that pan-neuronal expression of CG7442 RNAi-1 reduced mRNA levels to about 40% of the control (Figure 1E). Western blotting identified a strongly reacting protein with a mass of ~50kDa that was reduced to a level of ~75% of the control with pan-neuronal RNAi-1 expression (Figure 1F). These results confirm at the molecular level the expected reduction of CG7442 gene product with RNAi-1 expression.

Drosophila CG7442 overexpression impairs memory

We generated *UAS-CG7442* lines using the complete protein coding sequence to measure the effects of overexpression on olfactory memory. Two of these lines, #10 and #13, were molecularly characterized for changes of CG7442 at the mRNA and protein levels. We measured a ~4- and 10-fold elevation in mRNA, respectively, for *UAS-CG7442-10* and *UAS-CG7442-13* overexpression when driven by *N-syb-gal4* (Figure 2A). Using the anti-CG7442 antibody, we measured an increase in protein expression from *N-syb-gal4>UAS-CG7442-13* flies at a remarkable and unexpected 40-fold over the control (Figure 2B). Overexpressing CG7442 with two different MBn drivers produced a significant decrease in 3h memory (Figure 2C), without altering avoidance of odors or shock used during conditioning (Table S1). Combining the memory enhancing effect of CG7442 RNAi expression with the memory inhibiting effect of CG7442 overexpression produced a mutual suppression of the opposing phenotypes (Figure 2D). These results indicate that olfactory memory expression is controlled bidirectionally by the levels of CG7442 protein in the MBn.

CG7442 is a *Drosophila* organic cation transporter of the SLC22A family

Drosophila CG7442 is classed as a member of the SLC22A family due to its high homology throughout its amino acid sequence to mammalian SLC22A members and phylogenetic analyses (Figure S1,2). The closest human relatives based on pair-wise comparisons include SLC22A1-3 with ~30% amino acid sequence identity and ~50% sequence similarity, but strong similarity was also found with SLC22A4, 5, 15 and 16. Mammalian SLC22A1-5 and A16 have been characterized as organic cation transporters (OCT); *Drosophila* CG7442 is more distantly related to the SLC22A family members that transport organic anions (OAT), including SLCA6-13 (Figure S2). These observations suggest that organic cations rather than anions may be the favorable substrates for *Drosophila* CG7442. Signature amino acid motifs of mammalian SLC22A proteins are conserved in CG7442, including the 12 predicted transmembrane domains (TM), an extracellular loop between TM1-2 of ~100

amino acids, a large intracellular loop of ~70 amino acids encoded by sequences between TM6-7, the ASF (amphiphilic solute facilitator) motif at residues (146–161) and the MFS (major facilitator superfamily) motif connecting TM2 and TM3 (Burckhardt and Wolff, 2000). Other characteristic sequences of SLC22A proteins include the LPESVRWLL motif at residues 296–304 and the SEIYPTNLRN motif at residues 471–480 (Figure S1). Four out of six cysteine residues residing in the large extracellular loop required for oligomerization through disulfide bond formation and proper membrane targeting were also conserved in CG7442 (Figure S1; Keller et al., 2011). Furthermore, five different amino acids within TM4 of the rat SLC22A1 are required for transport of the general substrates, tetraethylammonium (TEA) and methyl-4-phenylpyridinium (MPP+; Popp et al., 2005); mutating any of these five amino acids abolishes transport activity. Three of these are conserved in the *Drosophila* CG7442 sequence [S227 (rS214), E240 (rE227) and V242 (rV229)], and the two others contain neutral amino acid substitutions [T233 (S→T) and I257 (L→I)]. Overall, sequence homology and functional motifs identified *Drosophila* CG7442 as a SLC22A family member that likely transports organic cations. Therefore, CG7442 will be referred to as DmSLC22A throughout the remainder of this report.

DmSLC22A is expressed in the MB calyx

We studied the spatial expression pattern of DmSLC22A by immunohistochemistry using an affinity purified polyclonal antibody. Marked expression was observed in a few specific brain regions, including the antennal lobe, the protocerebral bridge, and the MB calyx, along with the large fibers of the median bundle and optic tract (Figure 3A–B′). Although we observed pronounced staining within the calyx of the MB (Figure 3A, B), there was an unexpected lack of immunoreactivity within the MB lobe neuropil (Figure 3A′, B′, C–C″).

The expression pattern within the calyx as revealed by both confocal and super-resolution microscopy using two independent antibodies was especially unique and interesting. The staining occurred within distinct fibers, generally enveloping the calyx although some fibers were observed to run through the central region of the calyx (Figure 3D–D″, S3F–H). One interpretation for this pattern is that DmSLC22A is expressed in the MB cell bodies and trafficked specifically to their dendrites for function. High resolution images of the calyx border (Figure 3E–E″) showed that DmSLC22A immunoreactivity opposed the anti-Brp^{nc82} puncta, a presynaptic marker, and often surrounded it. These puncta probably define in large part the presynaptic terminals from antennal lobe Pn.

To test the possibility that the anti-DmSLC22A staining in the calyx represents mushroom body dendritic terminals, we quantified the immunoreactive signal in both control flies and flies with MB-targeted knockdown and overexpression, using the signal observed in the optic lobes to normalize the measurements (Figure 4A–C). We measured a ~50% and 30% reduction in DmSLC22A immunoreactivity in *238Y-gal4>CG7742-RNAi-1* and *R13F02-gal4>CG7742-RNAi-1* flies, respectively (Figure 4C). We performed the same immunohistochemical quantitation for flies overexpressing DmSLC22A and measured a 2.5-fold increase in calyx expression (Figure 4D–F).

We noticed in our analysis of the expression in the calyx that the DmSLC22A signal was reminiscent of a glial pattern (Doherty et al., 2009). To test an alternative possibility that

DmSLC22A is expressed primarily in glia, we performed immunohistochemistry using anti-DmSLC22A antibody on flies expressing GFP in all-glia, cortex-glia, ensheathing-glia and in astrocytes. We failed to observe significant signal overlap of DmSLC22A immunoreactivity in the calyx with the GFP signal representing these glia (Figure S3), providing no support for the hypothesis that the primary expression site of DmSLC22A is in MB-associated glia. This observation is consistent with the failure to detect a behavioral function for DmSLC22A in glia (Figure 1A). We did observe a dense, crescent-shaped region of immunoreactivity in the optic lobe that largely co-localized with the *repo*-GFP signal, a pan-glial marker (Figure S3D), suggesting a potential glial localization and function of DmSLC22A for visual processing. One homolog of DmSLC22A, mouse OCT3, is expressed in the sub-retinal space for the clearance of histamine (Rajan et al., 2000). Histamine is also the major insect neurotransmitter utilized by photoreceptor cells.

In agreement with the functional requirement for DmSLC22A in the α/β and α′/β′ MBn, we observed that the anti-DmSLC22A immunoreactive signal was co-localized with GFP reporters for the α′/β′ and α/β MBn (Figure S4). There was only slight overlap with GFP signal representing γ MBn. Therefore, we conclude that the primary loci of expression and function are the α′/β′ and α/β MBn.

The DmSLC22A memory suppressor function occurs from adult expression

We utilized the TARGET ($GAL80^{ts}$) system to control RNAi expression across time to determine whether the DmSLC22A memory suppression is a consequence of developmental or adult expression. Flies carrying *tub-gal80^{ts}, 238Y-gal4,* and either *CG7442-RNAi-1* or *UAS-CG7442-13,* were shifted between 18 and 30°C to repress or derepress GAL4 activity, respectively. When the flies containing the RNAi construct were kept at 30°C across development and into adulthood, enhanced memory expression was observed (Figure 5A). This was also observed when $GAL80^{ts}$ activity was derepressed only during adulthood. Similarly, an impaired memory phenotype was observed when DmSLC22A was over-expressed only during adulthood (Figure 5B). There was no consequence of expressing the RNAi or the cDNA during developmental periods. These experiments definitively show that knockdown or overexpression produces memory phenotypes due to expression in the adult organism.

DmSLC22A regulates both memory acquisition and retention

Next we asked whether the memory suppression phenotype was produced by altering memory acquisition or retention. Flies were trained with odor and a varying number of shock pulses and immediately tested after the last shock pulse in order to probe the rate of memory acquisition. Surprisingly, although the control genotype reached an asymptotic performance index after only three-shock training, the DmSLC22A knockdown flies required seven-shock training to reach this value. In other words, these data suggest that the rate of learning is impaired in the knockdown flies (Figure 5C). We observed this same acquisition impairment when DmSLC22A was inhibited using a second MBn driver, *R13F02-gal4,* and a α′/β′ MBn-specific driver, *c305-gal4* (Figure S5A). With 7–12 shock pulses during training, both control and experimental genotypes reach ceiling levels of performance (Figure 5C).

We tested memory retention after 12-shock training to measure the rate of memory decay. As illustrated in Figure 5D, the memory retention curves for control and experimental genotypes are parallel and qualitatively similar, but quantitatively dissimilar, with the DmSLC22A knockdown flies exhibiting enhanced performance at 1, 3, and 9h after conditioning. This enhancement was striking, approximating a doubling in performance at 9h. Memory performance a few hours after conditioning is experimentally separable into two major components: a component that can be disrupted with cold shock and a component that is resistant to this insult. We measured the cold-shock sensitive and resistant components by imposing a brief cold shock treatment at 1.5h after conditioning and testing performance at 3h. As expected, the DmSLC22A knockdown flies exhibited enhanced performance without cold shock compared to the control (Figure S5B). They also showed enhanced performance after cold shock, indicating that the knockdown enhanced both cold-shock sensitive and resistant forms. Thus, although impaired in the rate of acquisition compared to the control genotype (Figure 5C), training the DmSLC22A knockdown flies to ceiling levels of performance produces a more persistent memory consisting of both cold-shock resistant and sensitive components (Figure 5D, S5B). Putting this conclusion back into the context of the normal fly, DmSLC22A expression in the MBn speeds acquisition and suppresses the strength of memory produced, judged by the elevated and more persistent memory in the knockdown flies produced by conditioning to ceiling levels of performance (Figure 5D, F).

An alternative possibility is that the memory traces formed during acquisition in the knockdown flies become similar in strength to control flies, but DmSLC22A functions in post-acquisition processes of memory stability or expression. We probed this alternative hypothesis by measuring the rate of memory decay after normalizing the initial performance of control and experimental flies using reduced training intensity for the experimental flies. The results of this experiment show that the memory decay rate is identical between the two groups after this normalization (Figure 5E). We also performed a series of memory interference assays to probe deeper into the alternatives, predicting that stronger memory traces instilled during acquisition would enhance proactive interference and diminish retroactive interference. Proactive interference produced by learning a contingency between odor pairs C/D and electric shock immediately prior to learning an A/B contingency impaired A/B memory in control animals tested immediately afterwards by about 30% (Figure 5G). In contrast, the magnitude of this interference was greater than 45% in the DmSLC22A knockdown group, showing that proactive interference produced by the memory of the C/D contingency is more robust in this group. It should be noted that this effect is rapid; proactive interference inhibits new acquisition within minutes afterwards. This observation lends support to the conclusion that memory traces formed at acquisition in DmSLC22A knockdown animals are stronger than in controls. Consistent with this conclusion, retroactive interference produced by learning a C/D odor contingency after A/B was less robust in the knockdown group than in the control group (Figure 5H), consistent with the existence of a stronger A/B memory trace. These results strongly support the conclusion that DmSLC22A knockdown instills a stronger memory trace during acquisition (Figure 5F).

Yet another explanation for the elevated memory in the DmSLC22A knockdown flies is that they may be impaired in active forgetting (Shuai et al., 2010; Berry et al., 2012). A good way to test the forgetting hypothesis is to employ transgenes that express variants of the small GTPase Rac, since constitutively active Rac causes forgetting and dominant negative Rac inhibits it (Shuai et al., 2010). Flies were constructed to contain both the DmSLC22A RNAi transgene that enhances memory expression, and a Rac^{v12} expressing transgene that promotes forgetting (Shuai et al., 2010). The memory performance of the genotype was intermediate between the RNAi-expressing flies and the Rac^{v12} expressing flies (Figure S5C). Thus, expression of Rac^{v12} is not epistatic to the effects of DmSLC22A RNAi, nor is DmSLC22A RNAi expression epistatic to Rac^{v12}. This indicates that DmSLC22A knockdown functions in a pathway other than the forgetting pathway defined by Rac, producing an additive phenotype.

Cholinergic compounds are the preferred substrate for DmSLC22A

We prepared a stable HEK293 cell line with DmSLC22A expression inducible with doxycycline to identify substrates potentially transported by this protein. We observed strong, doxycycline-dependent expression of DmSLC22A as assayed by western blotting and immunohistochemistry compared to cells without doxycycline (Figure S6A, B). DmSLC22A was properly targeted to the plasma membrane and concentrated in focal adhesions.

We then utilized the doxycycline-induced cells expressing DmSLC22A to survey potential substrates for this transporter. The battery of compounds we tested included compounds previously identified as substrates for mammalian OCTs, including serotonin, dopamine, octopamine, histamine, acetylcholine, choline, betaine, and the general substrates for these transporters, MPP and TEA (Koepsell, 2013b). Known substrates for OCT6 and mOCTN1-2, spermidine and L-carnitine, were included in the assays. We also considered known neurotransmitters used for communication with MBn, which include acetylcholine, dopamine, serotonin, and octopamine (Pech et al., 2013). We assayed each substrate using both induced and un-induced cells in order to measure the transport activity above that from endogenous transporters in HEK293 cells.

Our results reveal that 9 of the 11 compounds tested can serve as substrates for DmSLC22A expressed in HEK293 cells (Figure 6). Those compounds that failed as substrates included octopamine and spermidine (Figure S7). The other nine compounds tested exhibited significant substrate activity, but three of the compounds showed an interesting uptake profile in which the transport activity of un-induced cells at later assay times exceeded that of the induced cells. These included TEA, betaine, and L-carnitine. This unexpected observation must be due to the DmSLC22A transporter interfering in some way with the transporters endogenously expressed by HEK293 cells, or by conferring bidirectional transport of substrates (Koepsell, 2013). Of particular interest were the cholinergic compounds and dopamine, since these specific substrates exhibited continuously increased transport in induced vs un-induced cells (Figure 6J).

We confirmed the substrate specificity of DmSLC22A using dissociated neurons from the adult fly brain for the assays, employing control neurons (*N-syb-gal4>+*), neurons

overexpressing DmSLC22A (*N-syb-gal4>CG7442*), and neurons expressing the DmSLC22A RNAi transgene (*N-syb-gal4>CG7442-RNAi)* (Figure S8). Our results indicate that DmSLC22A in *Drosophila* neurons transports MPP, TEA, choline, acetylcholine, betaine, histamine, and dopamine but not spermidine, serotonin, octopamine or carnitine. There was excellent correspondence in the results using knockdown vs overexpressing neurons.

We varied the substrate concentration across a range of about an order of magnitude (Figure 6K) in assays within their linear phase using both HEK293 cells and adult *Drosophila* neurons in order to determine the relative K_m and V_{max} for each substrate (Table S2). Our results show that choline and acetylcholine are transported with low μM Km values, while dopamine was transported with a Km of ~10 μM. The combined results indicate that choline and acetylcholine are the preferred substrates based on K_m and on transport efficiency (V_{max}/K_m).

DmSLC22A modulates memory strength by regulating cholinergic neurotransmission in the MB calyx

The identification of substrates for DmSLC22A prompted us to test the biological role for three neurotransmitters – acetylcholine, dopamine, and histamine – in memory expression. We began by feeding flies precursors to these neurotransmitters and measuring memory, after feeding, in control, knockdown, and flies overexpressing the transporter in the MBn. We predicted that increasing the levels of the primary neurotransmitter substrate used *in vivo* for regulating memory via DmSLC22A through dietary supplementation would improve memory in control flies, and knockdown of the transporter would phenocopy these behavioral gains. In addition, we predicted that overexpression of the transporter would limit behavioral memory in control flies, and that this could be partially reversed by increasing the levels of the relevant neurotransmitter through dietary supplementation. These predictions were made based on a synaptic model for the transporter effects: Reducing the DmSLC22A transporter at the synapse would allow its cognate neurotransmitter to have more persistent and stronger effects, while overexpressing the transporter would limit the magnitude and duration of the cognate neurotransmitter's actions. Dietary supplementation would provide for increased levels of neurotransmitter released at the relevant synapses.

Flies were starved overnight and fed with neurotransmitter precursors for 12h followed by conditioning and memory testing (Figure 7A–C). Supplementing food with L-Dopa or histidine impaired memory in control flies. The behavioral gains due to supplementing the DmSLC22A knockdown flies with these precursors were quantitatively similar to those observed using control flies, consistent with the conclusion that precursor supplementation produces behavioral effects through pathways independent of DmSLC22A. In contrast, choline supplementation improved behavioral performance in control flies. DmSLC22A knockdown in choline-supplemented flies produced levels of performance similar to those with the DmSLC22A knockdown only, possibly due to saturating the acetylcholine receptor from nutritional supplementation alone. These results are compatible only with the model that DmSLC22A knockdown improves memory by choline/acetylcholine transport. Moreover, overexpression of DmSLC22A in the MBn impaired memory, and dietary

supplementation with choline partially reversed this impairment (Figure 7D). Dietary supplementation of L-dopa or histidine to overexpressing flies produced further impairment in memory beyond the effects of the DmSLC22A transgene expression itself (Figure 7E, F).

Four observations led to the specific hypothesis that altered acetylcholine neurotransmission at the Pn:MBn synapse might underlie the memory gains observed in the DmSLC22A knockdown flies (Figure 8A): (i) Knockdown of DmSLC22A in the MBn produced the enhanced memory phenotype. (ii) DmSLC22A is preferentially expressed in the dendrites of the MBn. (iii) Dietary supplementation experiments described above fingered cholinergic transmission as the probable variable underlying memory suppression. (iv) The neurons presynaptic to MBn (Pn) are known to be cholinergic in their nature (Yusuyama et al., 2002; Gu and O'Dowd, 2006).

We challenged this hypothesis by testing two strong predictions that follow from the model. First, increasing/decreasing the abundance of DmSLC22A in the MBn should produce an inverse response in calcium influx in the MBn dendrites when flies are presented with odor stimulation. This is the consequence of increasing or decreasing the neurotransmitter persistence at the synapse by facilitating or reducing its transport from the synapse. Second, reducing the enzymatic pathway for terminating the acetylcholine signal at the Pn:MBn synapse by reducing acetylcholinesterase synthesized and released synaptically by the Pn should enhance memory expression in ways similar to DmSLC22A knockdown in the MBn. In addition, this enhanced memory expression should be suppressed by increasing the transporter-mediated termination of the signal, obtained by overexpressing SLC22A in the MBn.

We tested the first prediction by expressing G-CaMP6.0f in the MBn and measuring the postsynaptic calcium response in their dendrites by *in vivo* functional imaging. Compared with the control group, DmSLC22A knockdown in the MBn produced a ~30% increase in GCaMP6.0f fluorescence when flies were presented with either octanol or benzyaldehyde (Figure 8B–D). In contrast, overexpressing the DmSLC22A transporter in the MBn produced a ~30% decrease in the dendritic calcium response to odors (Figure 8E–G). These observations are congruent with the model that DmSLC22a provides a transport-mediated pathway for terminating cholinergic transmission at the Pn:MBn synapse.

We then tested the model by genetically manipulating cholinergic transmission specifically at the Pn:MBn synapse and measuring the effects on memory expression. Expression of an RNAi transgene to acetylcholinesterase in the Pn to reduce the enzymatic destruction of ACh at the Pn:MBn synapse using two different Pn drivers (*GH146-gal4* and *NP225-gal4*) enhanced 3h memory performance by 25–50% (Figure 8H, S5D). This observation is consistent with the model that increased ACh levels at that synapse enhances olfactory memory. In contrast, overexpression of DmSLC22A in the postsynaptic compartment to increase transport of ACh into MBn impaired memory expression (Figure 8H, S5D, 2C). When combined, these two genetic manipulations were mutually suppressive. These data, produced by specifically manipulating these pre- and post-synaptic partners in the fly, provide exceptionally strong evidence for the model that cholinergic neurotransmission is terminated by a balance between enzymatic destruction and transport mechanisms, and that

the memory suppression function of DmSLC22A is due to its transport role at the Pn:MBn synapse (Figure 8A).

DISCUSSION

Our data, provided above, connect the SLC22A family of transporters and memory suppression through the mechanism illustrated in Figure 8A. DmSLC22A, located on the dendrites of the adult α/β and α′/β′ MBn, removes ACh from the Pn:MBn synapses in the calyx. The normal expression level of this plasma membrane transporter limits the transference of olfactory information to the MBn by removing neurotransmitter from the synapse. Overexpression of DmSLC22A hardens this limit, weakening the CS representation and weakening memory formation. Reducing DmSLC22A expression has the opposite effect of softening the limit, producing a stronger CS representation and stronger memory formation. Thus, the data indicate that acetylcholinesterase and postsynaptic SLC22A transporter function jointly to regulate neurotransmitter persistence at the synapse. This conclusion is notable, given the longstanding emphasis on ACh degradation as the primary route for termination of the cholinergic synaptic signal. Although the evidence is strong for the proposed mechanism shown in Figure 8A, the transporter exhibits broad substrate specificity and expression outside of the Pn:MBn synapse. Alternative or additional mechanisms of action in memory suppression thus remain a possibility.

The current data are consistent with the model that ACh persistence at the Pn:MBn synapse is a surrogate for the strength of the CS and therefore a primary effector of olfactory memory strength. Other data similarly point to the strength of stimulation of MBn as an important variable for regulating memory strength. The MBn also receive inhibitory input through $GABA_A$ receptors expressed on the MBn. Overexpressing the MBn-expressed $GABA_A$ receptor, Rdl, impairs learning, while RNAi knockdown of this receptor in the MBn enhances memory formation (Liu et al., 2007). This regulation of memory strength is independent of the US pathway involved in classical conditioning, functioning similarly for both aversive and appetitive USs (Liu et al., 2009). However, we note that the *in vivo* functions for the SLC22A class of transporters must be broader than the focused model presented above. For instance, the data indicate that the *Drosophila* SLC22A protein transports both acetylcholine and dopamine in *ex vivo* preparations. Moreover, the protein's memory suppressor function maps to both MBn and the DAn. We have not yet explored how DmSLC22A might function in DAn to suppress memory formation, but one reasonable hypothesis following the logic in Figure 8 is that DmSLC22A transports acetylcholine at the synapse between upstream and putative cholinergic neurons that provide input to the DAn that convey the US in classical condition. Testing this hypothesis requires identifying the presynaptic neurons to the DAn that carry the US information.

One unexplained observation is that although DmSLC22A knockdown enhances the duration of memory produced from stronger memory traces instilled at acquisition, it slows the rate of acquisition as measured by acquisition curves. However, this observation has been made with another memory suppressor gene as well. A knockdown of the pre- and post-synaptic scaffolding protein, Scribble, has the same effect of producing more enduring memories but slowing acquisition (Cervantes-Sandoval et al., submitted). In addition, similar

observations have been made in mouse: injection of muscarinic acetylcholine receptor antagonists impairs memory acquisition but enhance retention (Easton et al., 2012).

Our studies bring a focus on the SLC22A family of plasma membrane transporters as potential targets for neurotherapeutics. Of the 24 members of this family, only a few have been studied in some detail in the nervous system. RNA expression experiments have shown that SLC22A1-5 are all expressed in the brain, with SLC22A3 and A4 being the most abundant (Alnouti et al., 2006, Cui et al., 2009), and immunohistochemistry experiments have revealed that SLC22A4-5 are localized at dendrites within the hippocampus (Lamhonwah et al., 2008). Mammalian members of this family of transporters and by extension, probably DmSLC22A, are subject to regulation by multiple signaling molecules including protein kinase A, calcium/calmodulin dependent protein kinase II, and the mitogen activated protein kinases (Wilde et al., 2009). Knockout mice for SLC22A2 and A3 show reduced basal level of several neurotransmitters in a region-dependent manner (Bacq et al., 2012; Vialou et al., 2008) and decreased anxiety-related behaviors (Wultsch et al., 2009, Courousse et al., 2015), although the effects of SLC22A3 on anxiety-related behaviors is debated (Vialou et al., 2008). In addition, the knockouts or antisense insults reveal behavioral changes in depression-related tasks, with SLC22A2 knockouts exhibiting increased behavioral despair, and SLC22A3 antisense-treated animals exhibiting decreased behavioral despair (Courousse and Gautron, 2015). Little is known about the biological or behavioral functions of the other members of the SLC22A family. Our results now show that the SLC22A family of transporters is also involved in memory suppression.

DmSLC22A is a unique and new type of memory suppressor gene. There are, to date, about two dozen memory suppressor genes identified in the mouse and about three dozen such genes in *Drosophila* (Lee, 2014; Walkinshaw et al., 2015). The mechanisms by which all of these genes suppress memory formation are not yet known, but a few themes that have emerged. For instance, several of the genes suppress memory formation by limiting excitatory neurotransmitter release and function, or the expression and function of post-synaptic receptors. DmSLC22A appears to fall into this category. Another example is Cdk5, which negatively influences the expression of NR2B and limits memory formation. Knockouts of some GABA receptors, mentioned above, reduce inhibitory tone of learning circuitry so as to facilitate memory formation. Several of the known memory suppressor genes are known to function in active forgetting processes. These include *damb*, a dopamine receptor involved in forgetting mechanisms (Berry et al., 2012); *scribble*, a pre- and post-synaptic scaffolding gene (Cervantes-Sandoval et al., submitted), and *rac*, a small G-protein involved in the biochemistry of active forgetting (Shuai et al., 2010). Memory suppressor genes can also encode signaling molecules that negatively regulate transcription factors required for long-term memory and the transcription factors themselves, such as repressing isoforms of *Aplysia* Creb (ApCreb2; Bartsch et al., 2000); ATF4, a transcription factor homolgous to ApCreb-2 (Chen et al., 2003); and protein phosphatase I (Genoux et al., 2002; Koshibu et al., 2011). Elucidating all of the genetic constraints on memory formation and their mechanisms will have profound consequences for understanding of how the brain forms and stores memories, and for the development of cognitive therapeutics.

EXPERIMENTAL PROCEDURES

Drosophila stocks used in this study are listed in Supplemental Experimental Procedures. Standard olfactory classical conditioning procedures were used in this study (Beck et al., 2000; Berry et al., 2012). These tests employed 2–4 day-old flies with odors delivered in an air stream and electric shock pulses (1.25s pulses every 5s at 90V) via a flexible copper grid. These procedures are detailed in Supplemental Experimental Procedures. Messenger RNA expression in control and DmSLC22a overexpression and knockdown flies was measured by qRT-PCR using standard procedures with glyceraldehyde 3-phosphate dehydrogenase (GAPDH) as a normalization control.

Polyclonal antisera were raised in guinea pigs against an *E. coli* expressed DmSLC22A:GST fusion protein. A mouse monoclonal antibody was prepared against the peptide sequence (DKLQQSSESRFP) found in the large intracellular loop connecting TM6 and TM7. Western blotting experiments were performed with the polyclonal antibody using standard procedures. Immunohistochemistry employing either the polyclonal or monoclonal anti-DmSLC22A antibody followed standard protocols except that dissected fly brains were re-fixed with 80% acetone after the paraformaldehyde fixation.

For transport assays, the open reading frame of CG7442 was cloned into the expression vector pcDNA ™5/FRT/TO (Invitrogen) and stable transformants were selected after transfection with this construct and pOG44. Single cell colonies were selected by limited dilution for further use. Radiolabeled potential substrates were incubated with the DmSLC22A-expressing HEK cells and the transport activity terminated by washing in ice-cold buffer. The cells were then solubilized and the internalized radioactivity counted. A similar experimental design was used to measure transport activity in *Drosophila* dissociated brain cells, except that the assays were performed with cell suspensions rather than monolayers and the cells pelleted by centrifugation for various wash steps.

Prism 5.0 was used for statistical analyses, with two-tailed t-tests for comparing two groups, and one-way ANOVA with a Tukey *post hoc* comparison for comparing multiple groups.

Supplementary Material

Refer to Web version on PubMed Central for supplementary material.

Acknowledgments

We thank Molee Chakraborty for assistance with immunohistochemistry experiments, and Trina Kemp for administrative help. Thanks to Marc Freeman for providing the glial-*gal4* lines. This study was supported by grants 2R37NS19904 and 2R01NS05235 from the NINDS to R.L.D. We also acknowledge the generosity of the Iris and Junming Le Foundation for their support in the purchase of a super-resolution microscope.

References

Abel T, Martin KC, Bartsch D, Kandel ER. Memory suppressor genes: inhibitory constraints on the storage of long-term memory. Science. 1998; 279:338–341. [PubMed: 9454331]

Alnouti Y, Petrick JS, Klaassen CD. Tissue distribution and ontogeny of organic cation transporters in mice. Drug Metab Dispos. 2006; 34:477–482. [PubMed: 16381671]

Aouida M, Poulin R, Ramotar D. The human carnitine transporter SLC22A16 mediates high affinity uptake of the anticancer polyamine analogue bleomycin-A5. J Biol Chem. 2010; 285:6275–6284. [PubMed: 20037140]

Ardiel EL, Rankin CH. An elegant mind: learning and memory in *Caenorhabditis elegans*. Learn Mem. 2010; 17:191–201. [PubMed: 20335372]

Bacq A, Balasse L, Biala G, Guiard B, Gardier AM, Schinkel A, Louis F, Vialou V, Martres MP, Chevarin C, et al. Organic cation transporter 2 controls brain norepinephrine and serotonin clearance and antidepressant response. Mole Psych. 2012; 17:926–939.

Bartsch D, Ghirardi M, Casadio A, Giustetto M, Karl KA, Zhu H, Kandel ER. Enhancement of memory-related long-term facilitation by ApAF, a novel transcription factor that acts downstream from both CREB1 and CREB2. Cell. 2000; 103:595–608. [PubMed: 11106730]

Beck CD, Schroeder B, Davis RL. Learning performance of normal and mutant *Drosophila* after repeated conditioning trials with discrete stimuli. J Neurosci. 2000; 20:2944–2953. [PubMed: 10751447]

Berry JA, Cervantes-Sandoval I, Nicholas EP, Davis RL. Dopamine is required for learning and forgetting in *Drosophila*. Neuron. 2012; 74:530–542. [PubMed: 22578504]

Blakely RD, Edwards RH. Vesicular and plasma membrane transporters for neurotransmitters. Cold Spring Harb Perspect Biol. 2012; 4:a005595. [PubMed: 22199021]

Burckhardt G, Wolff NA. Structure of renal organic anion and cation transporters. Am J Physiol -Renal Physiol. 2000; 278:F853–866. [PubMed: 10836973]

Chen A, Muzzio IA, Malleret G, Bartsch D, Verbitsky M, Pavlidis P, Yonan AL, Vronskaya S, Grody MB, Cepeda I, et al. Inducible enhancement of memory storage and synaptic plasticity in transgenic mice expressing an inhibitor of ATF4 (CREB-2) and C/EBP proteins. Neuron. 2003; 39:655–669. [PubMed: 12925279]

Courousse T, Bacq A, Belzung C, Guiard B, Balasse L, Louis F, Le Guisquet AM, Gardier AM, Schinkel AH, Giros B, et al. Brain organic cation transporter 2 controls response and vulnerability to stress and GSK3beta signaling. Mol Psychiatry. 2014; 20:889–900. [PubMed: 25092247]

Courousse T, Gautron S. Role of organic cation transporters (OCTs) in the brain. Pharmacol Ther. 2015; 146:94–103. [PubMed: 25251364]

Cui M, Aras R, Christian WV, Rappold PM, Hatwar M, Panza J, Jackson-Lewis V, Javitch JA, Ballatori N, Przedborski S, et al. The organic cation transporter-3 is a pivotal modulator of neurodegeneration in the nigrostriatal dopaminergic pathway. Proc Natl Acad Sci USA. 2009; 106:8043–8048. [PubMed: 19416912]

Davis RL. Mushroom bodies and *Drosophila* learning. Neuron. 1993; 11:1–14. [PubMed: 8338661]

Doherty J, Logan MA, Tasdemir OE, Freeman MR. Ensheathing glia function as phagocytes in the adult *Drosophila* brain. J Neurosci. 2009; 29:4768–4781. [PubMed: 19369546]

Easton A, Douchamps V, Eacott M, Lever C. A specific role for septohippocampal acetylcholine in memory? Neuropsychologia. 2012; 50:3156–3168. [PubMed: 22884957]

Genoux D, Haditsch U, Knobloch M, Michalon A, Storm D, Mansuy IM. Protein phosphatase 1 is a molecular constraint on learning and memory. Nature. 2002; 418:970–975. [PubMed: 12198546]

Gu H, O'Dowd DK. Cholinergic synaptic transmission in adult *Drosophila* Kenyon cells *in situ*. J Neurosci. 2006; 26:265–272. [PubMed: 16399696]

Guven-Ozkan T, Davis RL. Functional neuroanatomy of *Drosophila* olfactory memory formation. Learn Mem. 2014; 21:519–526. [PubMed: 25225297]

Havekes R, Abel T. Genetic dissection of neural circuits and behavior in *Mus musculus*. Adv Genet. 2009; 65:1–38. [PubMed: 19615530]

Keller T, Egenberger B, Gorboulev V, Bernhard F, Uzelac Z, Gorbunov D, Wirth C, Koppatz S, Dotsch V, Hunte C, Sitte HH, Koepsell H. The large extracellular loop of organic cation transporter 1 influences substrate affinity and is pivotal for oligomerization. J Biol Chem. 2011; 286:37874–37886. [PubMed: 21896487]

Koepsell H. Polyspecific organic cation transporters and their biomedical relevance in kidney. Curr Opin Nephrol Hypertens. 2013a; 22:533–538. [PubMed: 23852330]

Koepsell H. The SLC22 family with transporters of organic cations, anions and zwitterions. Mol Aspects Med. 2013b; 34:413–435. [PubMed: 23506881]

Koepsell H, Endou H. The SLC22 drug transporter family. Pflugers Arch. 2004; 447:666–676. [PubMed: 12883891]

Koshibu K, Gräff J, Mansuy IM. Nuclear protein phosphatase-1: an epigenetic regulator of fear memory and amygdala long-term potentiation. Neuroscience. 2011; 173:30–36. [PubMed: 21093547]

Lamhonwah AM, Hawkins CE, Tam C, Wong J, Mai L, Tein I. Expression patterns of the organic cation/carnitine transporter family in adult murine brain. Brain Dev. 2008; 30:31–42. [PubMed: 17576045]

Lee YS. Genes and signaling pathways involved in memory enhancement in mutant mice. Mol Brain. 2014; 7:43–57. [PubMed: 24894914]

Lin L, Yee SW, Kim RB, Giacomini KM. SLC transporters as therapeutic targets: emerging opportunities. Nat Rev Drug Discov. 2015; 14:543–560. [PubMed: 26111766]

Liu X, Krause WC, Davis RL. $GABA_A$ receptor RDL inhibits *Drosophila* olfactory associative learning. Neuron. 2007; 56:1090–1102. [PubMed: 18093529]

Liu X, Buchanan ME, Kyung-An Han KA, Davis RL. The $GABA_A$ receptor RDL suppresses the conditioned stimulus pathway for olfactory learning. J Neurosci. 2009; 29:1573–1579. [PubMed: 19193904]

Murakami S. *Caenorhabditis elegans* as a model system to study aging of learning and memory. Mol Neurobiol. 2007; 35:85–94. [PubMed: 17519507]

Nakamura T, Yoshida K, Yabuuchi H, Maeda T, Tamai I. Functional characterization of ergothioneine transport by rat organic cation/carnitine transporter Octn1 (slc22a4). Bio Pharm Bull. 2008; 31:1580–1584. [PubMed: 18670092]

Pech U, Pooryasin A, Birman S, Fiala A. Localization of the contacts between Kenyon cells and aminergic neurons in the *Drosophila melanogaster* brain using SplitGFP reconstitution. J Comp Neurol. 2013; 521:3992–4026. [PubMed: 23784863]

Rajan PD, Kekuda R, Chancy CD, Huang W, Ganapathy V, Smith SB. Expression of the extraneuronal monoamine transporter in RPE and neural retina. Curr Eye Res. 2000; 20:195–204. [PubMed: 10694895]

Shuai Y, Lu B, Hu Y, Wang L, Sun K, Zhong Y. Forgetting is regulated through Rac activity in *Drosophila*. Cell. 2010; 140:579–589. [PubMed: 20178749]

Stenesen D, Moehlman AT, Kramer H. The carcinine transporter CarT is required in *Drosophila* photoreceptor neurons to sustain histamine recycling. eLife. 2015; 4

Sturm A, Gorboulev V, Gorbunov D, Keller T, Volk C, Schmitt BM, Schlachtbauer P, Ciarimboli G, Koepsell H. Identification of cysteines in rat organic cation transporters rOCT1 (C322, C451) and rOCT2 (C451) critical for transport activity and substrate affinity. Am J Physiol-Renal Physiol. 2007; 293:F767–779. [PubMed: 17567940]

Tomchik, S.; Davis, RL. *Drosophila* Memory Research Through Four Eras: Genetic, Molecular Biology, Neuroanatomy, and Systems Neuroscience. In: Menzel, R.; Benjamin, P., editors. Invertebrate Learning and Memory. Elsevier; London: 2013. p. 359-377.

Vandenberg RJ, Ryan RR. Mechanisms of glutamate transport. Physiol Rev. 2013; 93:1621–1657. [PubMed: 24137018]

Vialou V, Balasse L, Callebert J, Launay JM, Giros B, Gautron S. Altered aminergic neurotransmission in the brain of organic cation transporter 3-deficient mice. J Neurochem. 2008; 106:1471–1482. [PubMed: 18513366]

Walkinshaw E, Gai Y, Farkas C, Richter D, Nicholas E, Keleman K, Davis RL. Identification of genes that promote or inhibit olfactory memory formation in *Drosophila*. Genetics. 2015; 199:1173–1182. [PubMed: 25644700]

Wilde S, Schlatter E, Koepsell H, Edemir B, Reuter S, Pavenstädt H, Neugebauer U, Schröter R, Brast S, Ciarimboli G. Calmodulin-associated post-translational regulation of rat organic cation transporter 2 in the kidney is gender dependent. Cell Mole Life Sci. 2009; 66:1729–1740.

Wultsch T, Grimberg G, Schmitt A, Painsipp E, Wetzstein H, Breitenkamp AF, Grundemann D, Schomig E, Lesch KP, Gerlach M, et al. Decreased anxiety in mice lacking the organic cation transporter 3. J Neural transm. 2009; 116:689–697. [PubMed: 19280114]

Yusuyama K, Meinertzhagen IA, Schürmann FW. Synaptic organization of the mushroom body calyx in *Drosophila melanogaster*. J Comp Neurol. 2002; 445:211–226. [PubMed: 11920702]

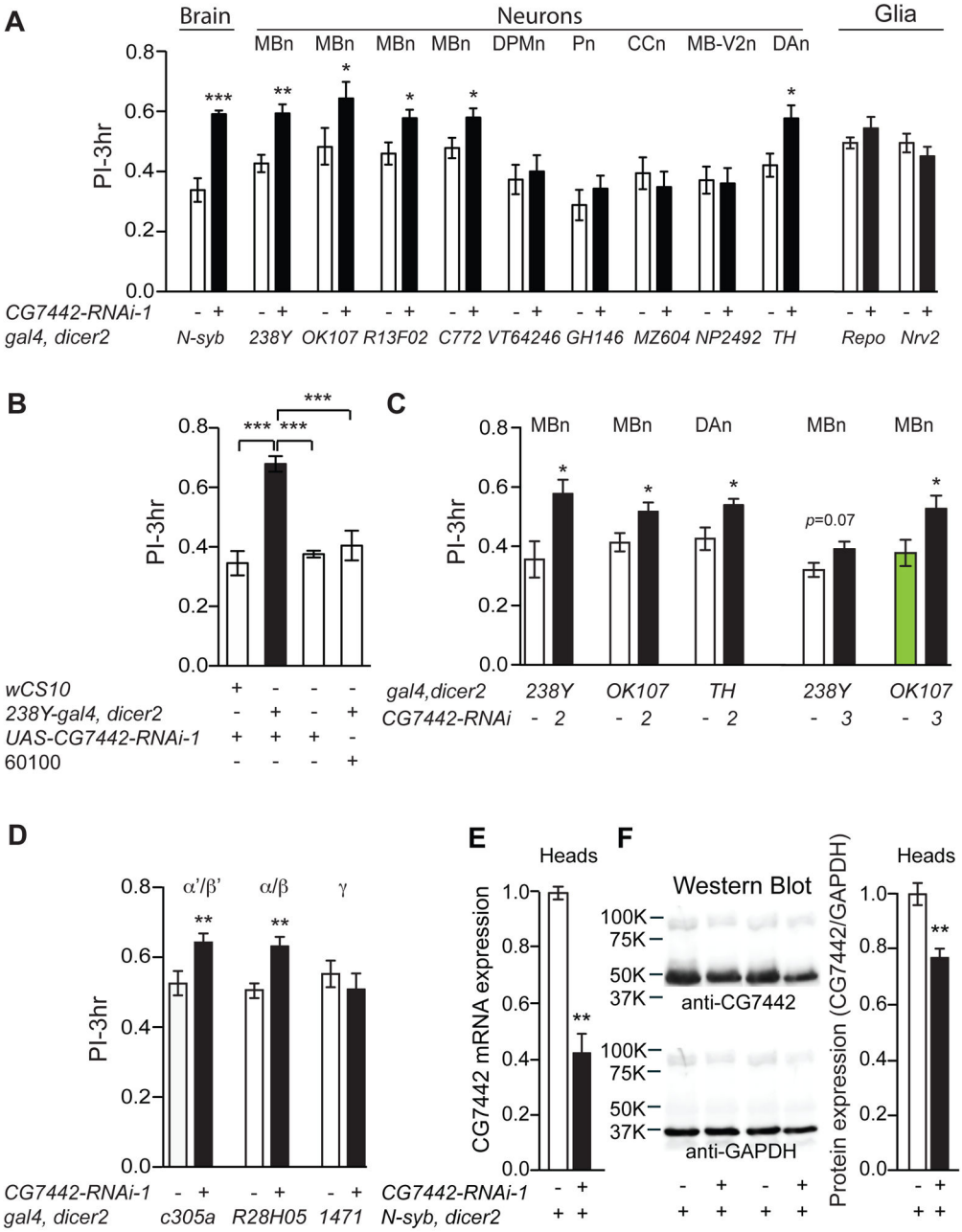

Figure 1. Memory suppression by CG7442 in MBn and DAn

(A) RNAi-1 targeting gene CG7442 was tested along with the corresponding genetic control line (*gal4*/60100) for effects on 3h olfactory memory (PI=Performance Index) using a battery of *gal4* drivers; *N-syb-gal4* (pan-neuronal), *238Y-gal4* (all MBn neurons), *OK107-gal4* (all MBn neurons), *R13F02-gal4* (all MBn neurons), *c772-gal4* (all MBn neurons), *VT64246-gal4* (DPMn), *GH146-gal4* (Pn), *MZ604-gal4* (CCn), *NP2492-gal4* (MB-V2n), *TH-gal4* (DAn), *repo-gal4* (pan glia), and *Nrv2-gal4* (cortex and subperineurial glia). **(B)** Memory enhancement with *238Y-gal4* occurred only in bigenic flies containing the *gal4* and RNAi-1 transgenes. **(C)** Memory expression was enhanced using two other RNAi transgenes

directed against CG7442, RNAi-2 and RNAi-3, confirming that the phenotype is due to CG7442 knockdown. **(D)** Memory expression was enhanced in flies expressing CG7442-RNAi-1 in the α′/β′ (*c305a-gal4*) and α/β (*R28H05-gal4*) MBn, but not in the γ MBn (*1471-gal4*). *Statistics for panels A, C, D:* Results are plotted as means ± SEM. Comparisons between each experimental group and its corresponding control group was performed using Student's t-test. N=6–8 for each group. **P*<0.05, ***P*<0.01, ****P*<0.001. *Statistics for panel B:* Results are plotted as the mean ± SEM. One-way ANOVA with Tukey's *post hoc* comparisons with ****P*<0.001. N=8 for each group. **(E)** Total RNA, extracted from the heads of control (*N-syb>60100*) and *N-syb*-driven *CG7442* knockdown flies was used for qRT-PCR experiments. A ~60% reduction of *CG7442* mRNA was measured in the knockdown flies. Triplicate measurements were performed on each of three biological replicates. *Statistics:* Results are plotted as the normalized mean ± SEM. Two-tailed student's t-test with ***P*<0.01. **(F)** Representative western blots of head lysates probed with polyclonal antisera against CG7442. Quantification of the immunoreactivity from both control and *N-syb* driven knockdown flies measured a ~25% reduction of CG7442 protein in the knockdown flies (right panel). GAPDH immunodetection was used as protein loading control. The CG7442 band intensity was compared to that for GAPDH and then the control normalized to 1.0. *Statistics:* Results are plotted as the normalized mean ± SEM. Two-tailed student's t-test with ***P*<0.01.

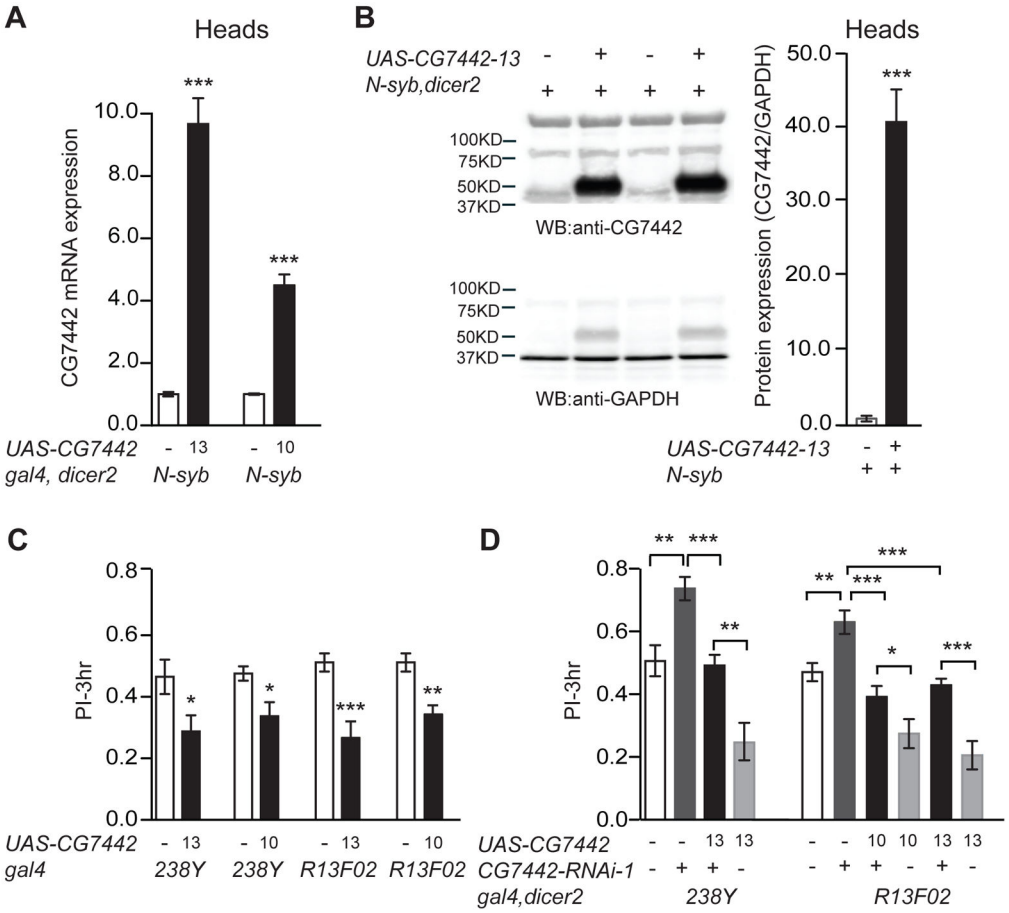

Figure 2. Memory impairment with CG7442 overexpression

(A) Quantitative RT-PCR analysis measured a 10- and 4-fold increase in CG7442 RNA in overexpression flies from lines 13 and 10, respectively. Total RNA was extracted from heads of *N-syb-gal4>wCS10* and *N-syb-gal4>CG7442* overexpression flies. Measurements in the overexpressing flies were obtained after normalizing the expression in control flies to 1.0. Experiments were performed in triplicate on each of three biological replicates. *Statistics*: Results are plotted as means ± SEM. N=3. Two-tailed student's t-test with ***P<0.001. **(B)** Representative western blots and quantification of CG7442 protein expression from *N-syb-gal4>wCS10* and *N-syb-gal4>CG7442*-13 heads. Whole head lysates were subjected to western blotting with anti-GAPDH detection as protein loading control. CG7442 protein expression was elevated by ~40 fold after normalizing to GAPDH expression (arbitrary units). *Statistics:* Results are plotted as the mean ± SEM. Two-tailed student's t-test with ***P<0.001. N=4 for each group. **(C)** Three-hour memory performance was significantly impaired with CG7442 overexpression in the MBn driven by *238Y-gal4* or *R13F02-gal4*, using both *UAS-CG7442-10* and *UAS-CG7442-13* transgenes. *Statistics:* Results are plotted as the mean ± SEM. One-way ANOVA analysis with Tukey's *post hoc* comparisons between the relevant groups with *P<0.05, **P<0.01, ***P<0.001. N=6–8 for each group. **(D)** Expression of *UAS-CG7442-10* or *UAS-CG7442-13* with two different MBn drivers (*R13F02-gal4* or *238Y-gal4*) fully rescued the enhanced memory phenotype produced by CG7442-RNAi-1 expression. *Statistics:* Results are plotted as means ± SEM. One-way

ANOVA analysis with Tukey's *post hoc* comparisons among the relevant groups with * $P<0.05$, ** $P<0.01$, *** $P<0.001$. N=6–8 for each group.

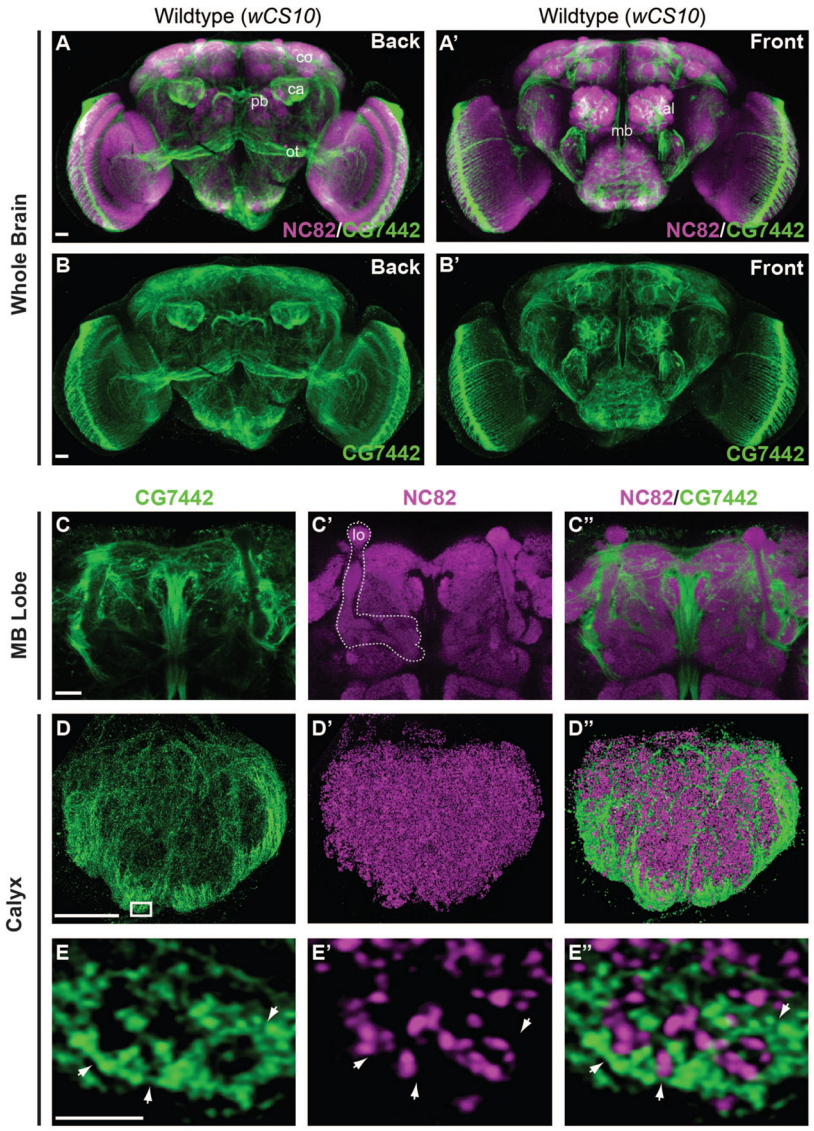

Figure 3. DmSLC22A is expressed in the MB calyx

(A–B′) Confocal views of the wild-type (*wCS10*) adult brain from the front and back decorated with anti-Brp^{nc82} (magenta) and anti-DmSLC22A (green). The distribution of DmSLC22A was strongest in the MB calyx (ca), cortex (co), antennal lobe (al), the ventral side of protocerebral bridge (pb), and the optic tract (ot). **(C–C″)** High magnification image of the MB lobes (lo, white outline) showing a lack of DmSLC22A expression. **(D–D″)** Super-resolution images of the MB calyx revealing distinct fiber tracts running through the calyx and DmSLC22A expression largely enveloping the ventral and lateral calyx. **(E–E″)** A 200nm thick slice of the ventral calyx (boxed region in **D**) showing the lack of overlap between DmSLC22A immunoreactivity and the presynaptic marker, Brp^{nc82}. Scale bar = 20μm in A–C″, 10μm in D–D″, and 1μm in E–E″.

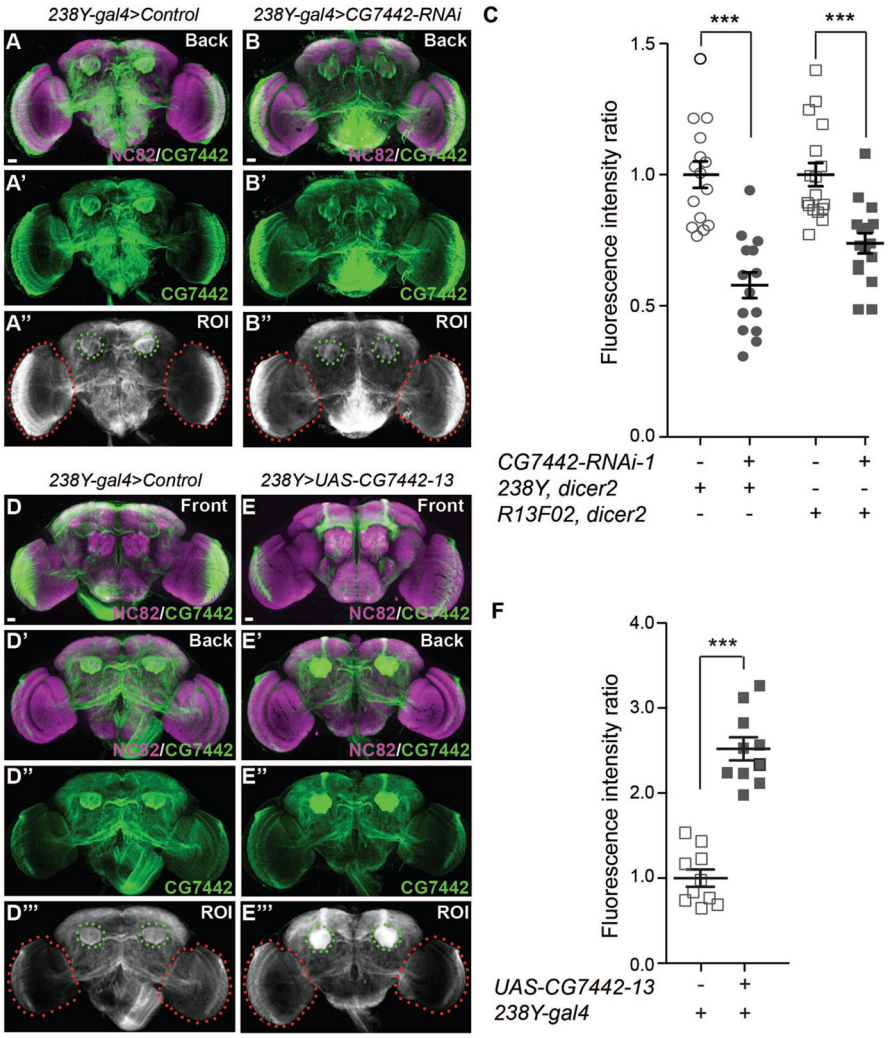

Figure 4. DmSLC22A knockdown and overexpression in the MB

(A–B″). Representative of whole brains co-labeled with anti-Brp^{nc82} (magenta) and anti-DmSLC22A (green) antibodies, for control and *238Y-gal4* driven knockdown flies. The region of interest (ROI) for quantification is illustrated in panels F″ and G″. **(C)** The signal from the calyx in each fly was normalized to the signal in the optic lobes and the fluorescence intensity ratio (calyx intensity)/(optic lobe intensity) for the control genotype was set to 1.0. The fluorescence intensity ratio was reduced by ~43% and 30% in DmSLC22A knockdown flies driven by *238Y-gal4* and *R13F02-gal4*, respectively. *Statistics:* Two-tailed student's t-test with ***P<0.001. N≥14. **(D–E‴)** Representative of whole brains co-labeled with anti-nc-82 (magenta) and anti-DmSLC22A (green) for control and *238Y-gal4* driven overexpressing flies. The region of interest (ROI) for quantitation of the signal is illustrated in panels I‴ and J‴. **(F)** The normalized signal increase in *238Y-gal4* driven DmSLC22A overexpression flies was ~2.5 fold. *Statistics:* Two-tailed student's t-test with ***P<0.001. N=10. Scale bar = 20μm in A–B″ and D–E‴.

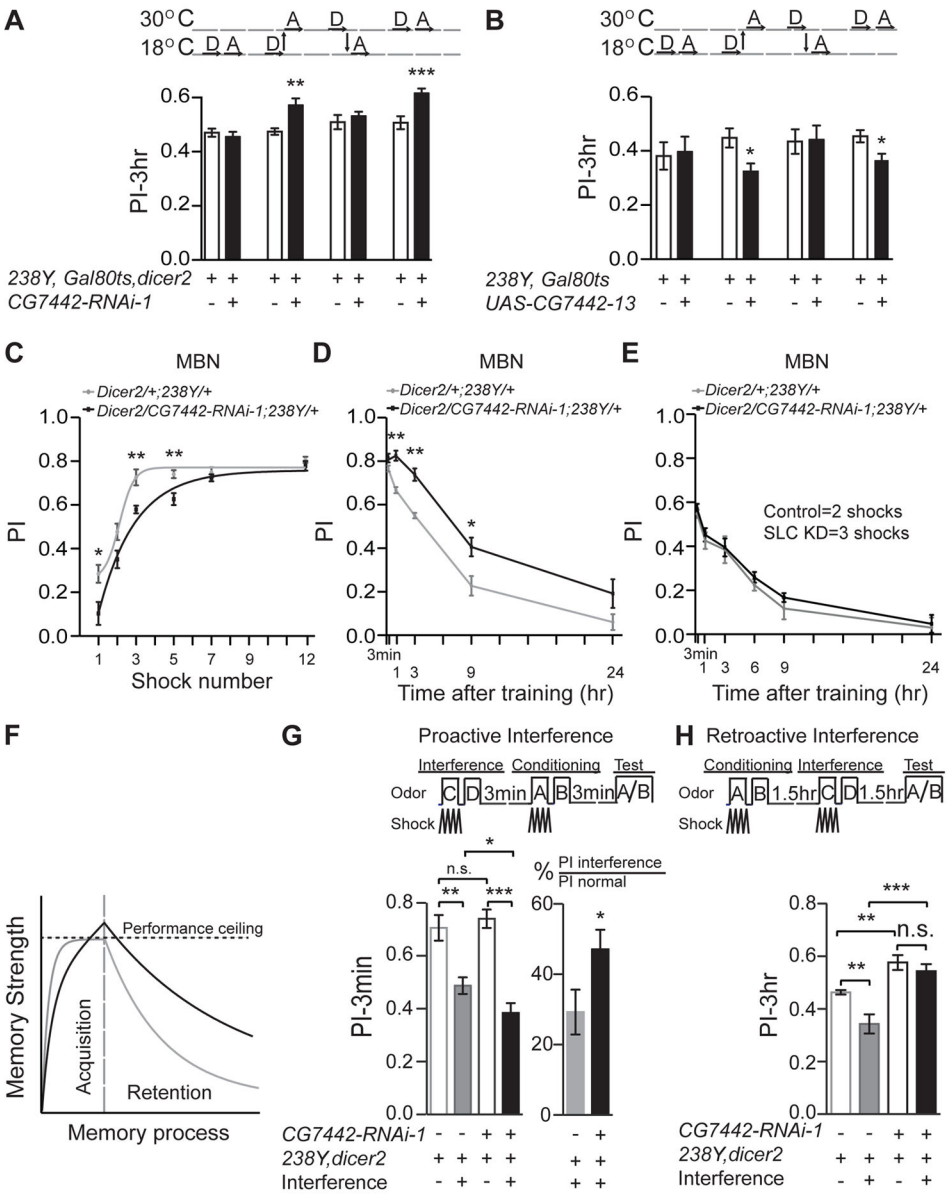

Figure 5. DmSLC22A is required during adulthood for normal memory acquisition and retention

(A, B) Shifting knockdown or overexpressing flies from 18° to 30°C at eclosion produced the memory phenotype observed with constant treatment at 30°C. D=Development, A=Adulthood. *Statistics:* Results are plotted as the mean ± SEM. Two-tailed student's t-test with **P*<0.05, ***P*<0.01, ****P*<0.001. N=8–12 for each group. **(C)** Memory acquisition using 1- to 12-shock training. **(D)** Memory retention after 12-shock training at time points up to 24h after conditioning. **(E)** Memory retention after normalizing initial acquisition. Control and DmSLC22a knockdown flies were trained with 2 and 3 shock pulses, respectively, providing for normalized initial performance at PI=0.56. Memory retention was measured from 3m to 24h conditioning. *Statistics for **C–E:*** Results are plotted as the mean ± SEM. Two-way ANOVA and Bonferroni posthoc analysis with **P*<0.05, ***P*<0.01. N=8–12

for each group. **(F)** Schematic diagram of acquisition rate and memory retention for control (gray) and DmSLC22A knockdown (black) flies, showing that the rate of acquisition is slowed in the knockdown flies but that the strength of memory produced during "saturation" training exceeds the control as well as the ceiling level of behavioral performance. **(G, H)** Effects of proactive and retroactive interference on memory performance. Proactive interference **(G)** was introduced prior to conditioning and 3m performance measured. The greater interference observed with the DmSLC22A knockdown flies indicates a stronger memory of the interference training. Retroactive interference **(H)** inhibited performance of the DmSLC22A knockdown less than the control genotype, indicating stronger memory of the initial conditioning event. *Statistics for **G, H***: Results are plotted as the mean ± SEM. One-way ANOVA with Tukey's *post hoc* comparisons with *$P<0.05$, ** $P<0.01$, *** $P<0.001$. N=8–12 for each group.

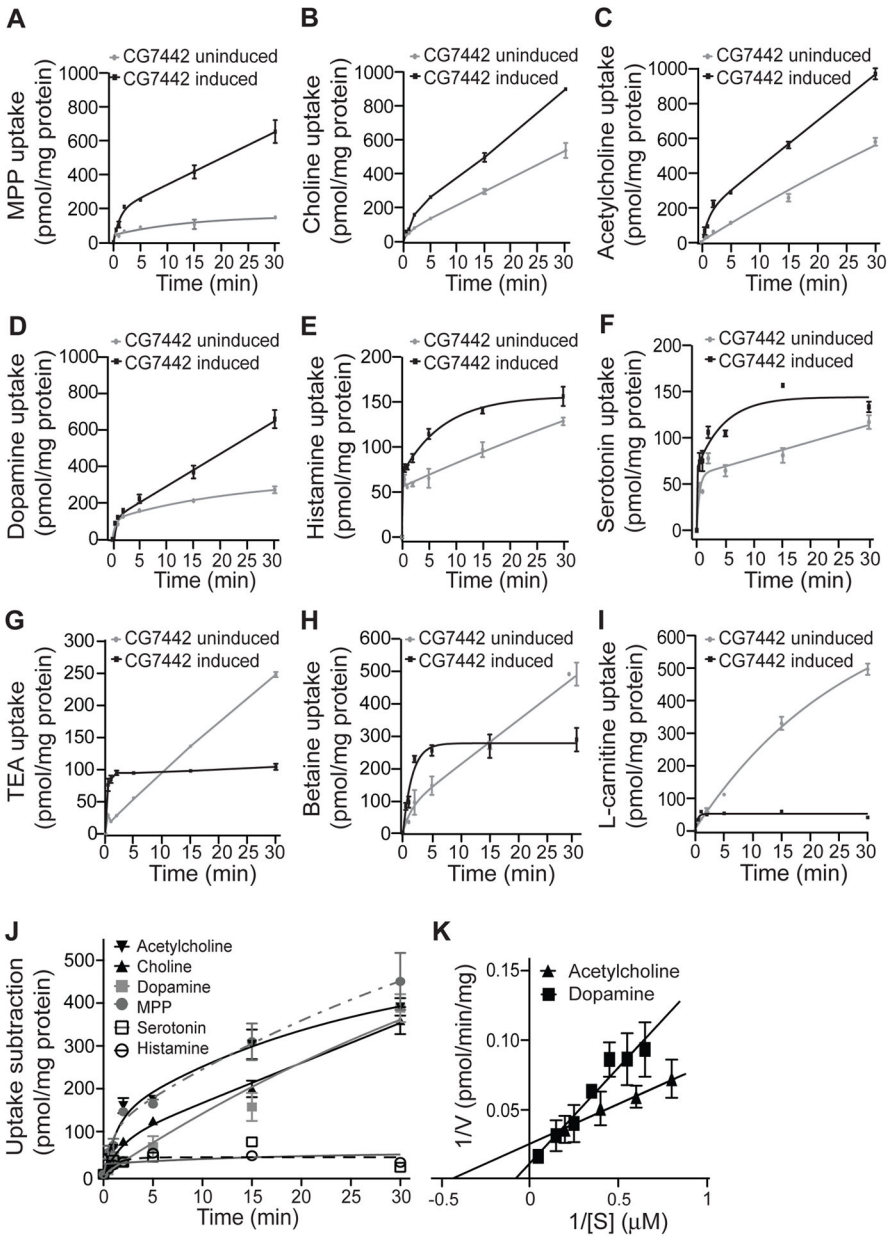

Figure 6. DmSLC22A substrates identified using engineered HEK293 cells

(A–K) Transport activity of candidate substrates in HEK293 cells. Expression of DmSLC22A was induced with 1.5 μg/ml doxycycline in experimental groups (black line) for 72 hours, while an untreated group (gray line) was used in parallel to measure basal activity. Intracellular content (pmol/mg total protein) of substrate was measured at multiple times to 30m after initiating the reaction. **(J)** Transporter activity measured in the uninduced cells was subtracted from the induced activity to measure the contribution due to DmSLC22A. Table S2 lists the apparent K_m and V_{max} values for each substrate. **(K)** Representative Lineweaver-Burk plots for acetylcholine and dopamine for calculation of K_m and V_{max} values. Panel K shows the average of three separate experiments with assays for each experiment being measured in triplicate. Three technical replicates were performed for

each substrate using three different biological samples. *Statistics:* Results are plotted as means ± SEM with * $P<0.05$, ** $P<0.01$.

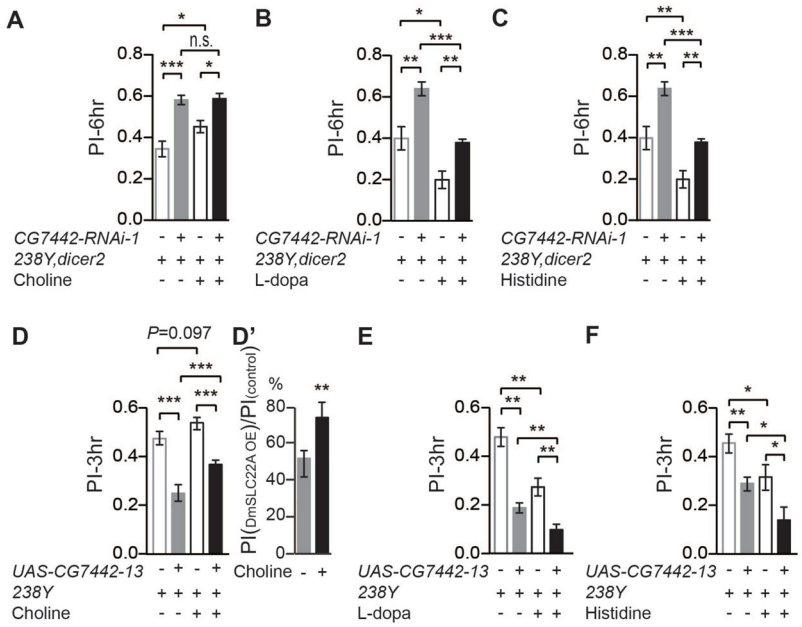

Figure 7. Effects of manipulating choline, dopamine and histamine levels on olfactory memory

Flies were constructed to knockdown the expression of DmSLC22A using *238Y-gal4* **(A–C)** or overexpress the transporter **(D–F)**. These flies and their control groups were fed the precursors to the neurotransmitters acetylcholine (choline) **(A, D),** dopamine (L-dopa) **(B, E),** and histamine (histidine) **(C, F).** Memory was tested at either 3 or 6h after conditioning. **(A)** Choline supplementation significantly improved memory in both control flies and knockdown flies, but did not take the performance of the knockdown flies to a level that exceeded the non-supplemented control group. In contrast, both L-dopa and histidine supplementation impaired the performance of both control and knockdown flies **(B, C). (D)** Overexpression of DmSLC22A impaired memory, and choline supplementation partially rescued this impaired performance. **(E, F)** L-dopa and histidine supplementation further impaired the performance of DmSLC22A overexpressing flies. *Statistics*: Results are plotted as means ± SEM with * $P<0.05$, ** $P<0.01$, *** $P<0.001$. One-way ANOVA analysis with Tukey's *post hoc* comparison. N=12 for all groups.

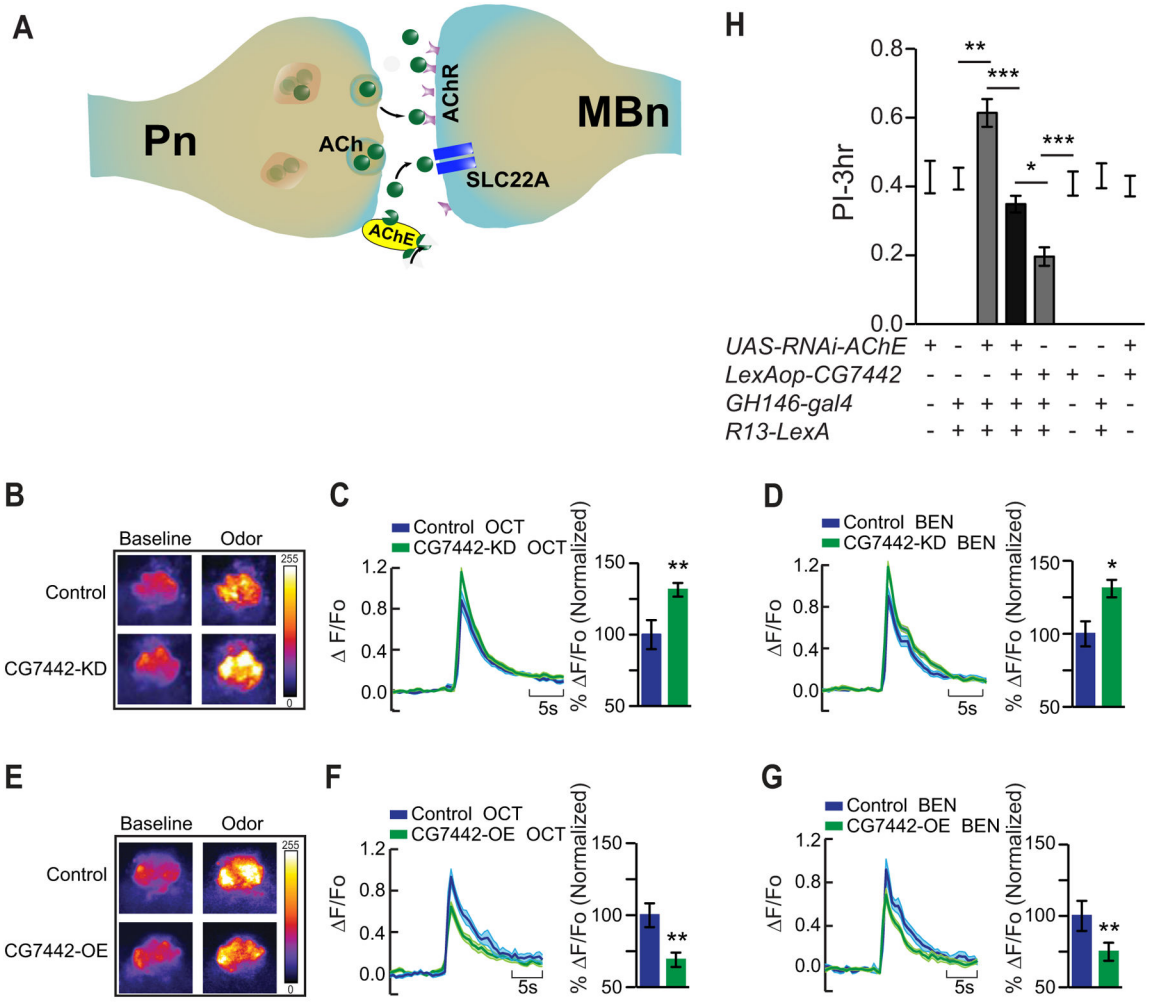

Figure 8. DmSLC22A regulates cholinergic neurotransmission at the Pn:MBn synapse for memory suppression

(A) Model for the role of DmSLC22A at the Pn:MBn cholinergic synapse. Acetylcholine (ACh) released from Pn in response to odor presentation activates it's postsynaptic partner, the MBn, through excitatory acetylcholine receptors (AChR). Acetylcholinesterase (AChE) at the synapse provides one pathway that terminates synaptic transmission by hydrolyzing acetylcholine. DmSLC22A provides a second pathway by transporting the released acetylcholine and choline into the MBn. Knocking down the expression of the transporter at the synapse leads to more persistent actions of ACh and stronger memory traces. Overexpression of the transporter has the opposite effect, prematurely terminating the actions of ACh leading to impaired memory. (**B**–**G**) Calcium responses in the MBn dendrites with odor presentation to control and experimental flies with reduced or increased DmSLC22A expression. (**B**, **E**) Representative pseudo-color images of GCaMP6.0^{f} fluorescence (%ΔF/F) obtain from *in vivo* functional imaging at baseline and during odor presentation to control, knockdown (KD) and overexpression (OE) flies. (**C**–**D, F**–**G**) GCaMP6.0^{f} responses from control and experimental flies across odor presentations of octanol (OCT) and benzaldehyde (BEN), with bar graph quantitation of the maximum

percentage change in signal relative to the control as normalized to 100%. (**B**–**D**) In response to odor-triggered Pn excitation, flies with reduced expression of DmSLC22A in the MBn (*R13F02-gal4)* showed a significant increase in GCaMP signal in the dendrites. (**E**–**G**) DmSLC22A overexpression in the MBn decreased the GCaMP signal obtained in response to odor presentation. *Statistics for* ***C, D, F, G***: Results are plotted as means ± SEM. Two-tailed student's t-test with * $P<0.05$, ** $P<0.01$. N=9–15 for all groups. (**H**) Genetic manipulation of cholinergic neurotransmission at Pn:MBn synapses. (**H**) Reducing AChE with RNAi expression in the Pn (*GH146-gal4)* enhanced memory expression, while overexpression of DmSLC22A in the MBn (*R13-LexA)* impaired memory expression. Overexpression of DmSLC22A in the MBn suppressed the enhanced memory expression due to AChE knockdown in the Pn. The genotypes of for the 2nd and 7th bars are *GH146-gal4;R13-LexA*>60100 and *GH146-gal4;R13-LexA*>8622, respectively. The 8622 line harbors the *P{CaryP}attP2* site, the docking site for the *LexAop* transgene. The former genotype serves as the control for RNAi expression; the latter as the control for *LexAop-DmSLC22A* expression. *Statistics:* Results are plotted as means ± SEM with * $P<0.05$, ** $P<0.01$, *** $P<0.001$. One-way ANOVA with Tukey's *post hoc* comparisons. N=7–9 for all groups.